International Journal of Safety and Security Engineering
Vol. 16, No. 5, May, 2026, pp. 969-983
Journal homepage: http://iieta.org/journals/ijsse

Consequence Analysis of Tetrahydrofuran Accidents in Storage and Road Transport: A High-Severity Hazard Assessment for Disaster and Emergency Management

Noor Khader Hussain Hussain, Sajjad Jokar, Sorush Saeedi, Mohammadreza Mohammadiahani, Esra Imer, Didem Saloglu*

Department of Disaster and Emergency Management, Disaster Management Institute, Istanbul Technical University, Istanbul 34469, Turkey

Corresponding Author Email: saloglu@itu.edu.tr

https://doi.org/10.18280/ijsse.160504

Received: 15 March 2026
Revised: 28 April 2026
Accepted: 22 May 2026
Available online: 31 May 2026

Keywords:
Areal Locations of Hazardous Atmospheres modelling, chemical transport risk, disaster risk reduction, emergency planning, tetrahydrofuran

ABSTRACT

The storage of volatile organic compounds (VOCs) poses significant challenges for disaster risk reduction (DRR) due to their combined toxic, fire, and explosion hazards. Tetrahydrofuran (THF), a highly volatile and flammable solvent widely used in industrial applications, presents particular concern in accidental release scenarios. This study evaluates the potential consequences of THF release incidents to support emergency preparedness and disaster risk management. A quantitative modelling approach was applied using the Areal Locations of Hazardous Atmospheres (ALOHA) 5.4.7 software to simulate accidental THF release scenarios under site-specific conditions in Kocaeli–Izmit, Türkiye. THF accident risks were assessed across four representative scenarios: toxic vapor dispersion, pool fire, storage-tank boiling liquid expanding vapor explosion (BLEVE), and road-tanker BLEVE. The study quantifies thermal radiation and explosion impacts to determine safety distances and potential consequences. The results indicate that, in the non-ignited release scenario, the ERPG-1 toxic concentration threshold (100 ppm) extends up to 98 m downwind, while ERPG-2 and ERPG-3 thresholds remain confined to the near-field region. In the pool fire scenario, thermal radiation impact distances reach 27 m at the 2.0 kW/m² threshold. For storage-tank BLEVE events, thermal radiation hazard distances extend to 112 m for 50% mass involvement and 139 m for 100% mass involvement; for the road-tanker BLEVE case, the maximum thermal radiation distance reaches 637 m under full mass involvement.

1. INTRODUCTION

The increasing scale and complexity of industrial activities involving hazardous chemicals have intensified the challenges faced by disaster management and disaster risk reduction (DRR) systems worldwide [1]. Among these challenges, accidents associated with the storage and surface transport of volatile organic compounds (VOCs) represent a critical concern due to their potential to trigger toxic releases, fires, and explosions with severe consequences for human health, infrastructure, and the environment. VOC-related incidents frequently evolve into multi-hazard events, where toxic exposure, thermal radiation, and blast effects can occur either independently or sequentially, complicating emergency response and risk mitigation efforts. As industrial supply chains expand and hazardous materials are stored and transported more frequently through urbanized and industrial corridors, the likelihood of such complex accident scenarios increases, underscoring the need for robust, scenario-based risk assessment approaches within the DRR framework [2, 3].

Tetrahydrofuran (THF) is a widely used VOC in petrochemical, pharmaceutical, and polymer industries, valued for its solvent properties and chemical versatility. However, its low boiling point, high vapor pressure, and flammability make it particularly hazardous in the event of accidental release [4]. Upon loss of containment, THF can rapidly evaporate, forming dense vapor clouds capable of posing both toxic inhalation risks and ignition hazards [5]. These characteristics position THF as a representative compound for examining the broader disaster risk implications associated with VOC storage and transport. From a disaster management perspective, understanding the potential impact zones associated with THF releases is essential for emergency planning, land-use management, and the protection of responders and nearby populations.

Industrial and transport-related chemical accidents have been repeatedly identified as significant contributors to technological disasters, particularly in regions experiencing rapid industrialization and infrastructure development [6]. Türkiye, and specifically industrial hubs such as Kocaeli-Izmit, exemplifies this challenge due to the concentration of chemical facilities, storage sites, and major transportation routes. The proximity of hazardous material transport operations to populated and industrial areas increase the potential for cascading effects, where an initial release may escalate into fire or explosion scenarios with wider spatial consequences [7]. In such contexts, DRR requires not only regulatory compliance but also the application of predictive

tools capable of quantifying hazard extents under realistic environmental and operational conditions.

Atmospheric dispersion and consequence modelling tools have become integral to emergency planning for hazardous material incidents. The Areal Locations of Hazardous Atmospheres (ALOHA) software, developed to support emergency response and risk assessment, enables the estimation of threat zones resulting from toxic releases and flammable scenarios. Such tools are widely used to evaluate potential exposure distances, thermal radiation impacts, and explosion effects under defined meteorological and site-specific conditions [8, 9]. Within the disaster management domain, these models support decision-making by translating chemical and physical properties into spatial representations of risk that are directly applicable to emergency response operations.

Despite the availability of modelling tools and regulatory guidance, gaps remain in the systematic evaluation of VOC-related disaster scenarios, particularly those involving combined toxic, fire, and explosion hazards during storage and surface transport [10]. Existing studies have frequently focused on stationary industrial installations or have examined individual hazard types in isolation [11]. Comparatively fewer investigations have addressed integrated multi-scenario assessments that consider the progression from non-ignited releases to fire and catastrophic explosion events within a single analytical framework. Moreover, the specific risks associated with THF storage vessels and their transport-related accident scenarios have received limited attention in the disaster risk literature, especially in the context of surface transport routes subject to varying meteorological and environmental conditions.

Another notable gap concerns the application of consequence modelling to support practical emergency planning parameters, such as safety distances and exclusion zones, tailored to realistic storage configurations and transport scenarios. While general hazard classifications for VOCs are well established, disaster management practitioners require location-specific and scenario-specific information to effectively plan response actions [11, 12]. The lack of detailed case-based assessments limits the ability of emergency planners to anticipate the spatial extent of toxic exposure, thermal radiation, and blast effects associated with accidental THF releases.

In response to these gaps, the present study focuses on the quantitative assessment of potential disaster scenarios arising from the accidental release of THF during storage and surface transport conditions representative of the Kocaeli–Izmit region. The study is situated within the broader DRR context, emphasizing the need to understand and quantify the potential consequences of technological hazards before an incident occurs. Rather than addressing prevention mechanisms or regulatory compliance in isolation, the study adopts a consequence-based perspective aligned with emergency preparedness and response planning objectives. In this context, the primary objective of this research is to evaluate the potential impacts associated with four representative THF accident scenarios: non-ignited toxic vapor dispersion, pool fire resulting from immediate ignition, storage-tank boiling liquid expanding vapor explosion (BLEVE), and road-tanker BLEVE. These scenarios represent escalating levels of severity commonly considered in disaster management planning for hazardous materials. By applying established modelling approaches under site-specific meteorological conditions, the study aims to delineate hazard zones relevant to human health and safety without introducing new assumptions beyond those defined in the existing modelling framework.

By addressing the combined toxic and physical hazards associated with THF storage and transport within a unified analytical framework, this study contributes to the disaster management literature by strengthening the link between chemical hazard modelling and practical DRR applications. The findings are positioned to enhance understanding of technological disaster risks associated with VOCs and to support more informed emergency planning in industrialized and transport-intensive regions.

2. METHODS

2.1 Study area and case description

This study is based on a representative industrial and transport-related accident scenario involving the release of THF in the Kocaeli–Izmit region of Türkiye. The location is situated at geographic coordinates 40°45′23.04″ N and 29°51′35.65″ E, with an elevation of approximately 5 m above sea level. The selected case study considers two representative configurations: a vertical cylindrical storage tank and a road chemical tanker used for THF transport. These configurations reflect typical industrial storage and surface transportation conditions encountered in hazardous material logistics.

2.2 Chemical properties and storage configuration

In this paper, THF is modelled as the hazardous substance of interest due to its widespread industrial use and hazardous physical properties.

Table 1. Chemical data of tetrahydrofuran (THF)

Parameter	Value
Chemical Name	THF
CAS Number	109-99-9
Molecular Weight	72.11 g/mol
ERPG-1	100 ppm
ERPG-2	500 ppm
ERPG-3	5000 ppm
IDLH	2000 ppm
LEL	20000 ppm
UEL	118000 ppm
Ambient Boiling Point	66.0 °C
Vapor Pressure at Ambient Temperature	0.13 atm
Ambient Saturation Concentration	128,420 ppm or 12.8%

Table 2. Storage tank data

Leak Source	Hole in Vertical Cylindrical Tank
Escaping Chemical	Flammable (not burning)
Tank Diameter	0.55 m
Tank Length	0.85 m
Tank Volume	202 L
Contents	Liquid
Internal Temperature	14 °C
Chemical Mass in Tank	144 kg
Tank Fill Level	80%
Circular Opening Diameter	10 cm
Opening Position from Bottom	0 m

The chemical and thermophysical properties used in this study are summarized in Table 1, while storage and transport configuration parameters are presented in Table 2.

2.3 Meteorological conditions

Meteorological conditions used in the modelling were defined based on site-specific parameters for the Izmit Port region and are summarized in Table 3. The ambient air temperature is specified as 14 °C, with a relative humidity of 68%. Wind conditions are defined by a wind speed of 3 m/s measured at a height of 10 m, with wind direction originating from the north-northeast (NNE). The atmospheric stability class is defined as Class C, representing slightly unstable conditions. Cloud cover is specified as four-tenths, and no temperature inversion height is assumed.

The ground roughness is classified as open country, and the building air exchange rate is defined as 0.57 air changes per hour, corresponding to an unsheltered single-story structure. These meteorological inputs are used consistently across all simulations and serve as boundary conditions for atmospheric dispersion, evaporation, fire, and explosion modelling within the ALOHA 5.4.7 framework. To ensure reproducibility of the study, the key ALOHA model settings and input assumptions are summarized in Appendix.

Table 3. Meteorological parameters of Kocaeli-Izmit, Turkiye

Location	Izmit Port, Turkiye
Coordinates	40º45'23.04"N, 29º51'35.65"E
Elevation	5 m
Building Air Exchanges Per Hour	0.57 (unsheltered single storied)
Parameter	Value
Wind	3 m/s from NNE at 10 m
Ground Roughness	Open country
Cloud Cover	4 tenths
Air Temperature	14 °C
Stability Class	C
Inversion	No inversion height
Relative Humidity	68%

2.4 Scenarios

This paper utilizes the ALOHA modelling framework to conduct a quantitative risk assessment (QRA) of THF release scenarios at a facility in Kocaeli-Izmit, Türkiye. The modelling evaluates the spatial and temporal impacts of four distinct accident trajectories, ranging from passive atmospheric dispersion to catastrophic thermal events. The following scenarios were systematically simulated to determine the safety perimeters and potential impact on human health and infrastructure:

Scenario 1—Passive dispersion (toxic vapor cloud of tetrahydrofuran)

In this scenario [13], THF leaks from the storage tank through a 10 cm breach but does not encounter an ignition source. An evaporating puddle forms without burning following leakage. As a result, its tank failure type can be defined as a vertical cylindrical storage tank that leaks flammable liquid under pressure without burning chemically by forming an evaporating puddle.

Investigation of explosion damage, death and minor injury radius for vapor cloud explosion (VCE) of THF using TNT equivalence formula. The investigation of explosion effects, particularly the assessment of damage, fatality, and injury radius, is a critical aspect of chemical safety and risk management. THF, a widely used organic solvent, exhibits significant flammability and explosive potential under certain conditions. Evaluating the blast consequences of THF VCEs requires a quantitative approach, commonly employing the TNT equivalence method. This method enables the estimation of overpressure effects and the corresponding distances at which structural damage, fatalities, and minor injuries are likely to occur, facilitating effective hazard mitigation and emergency planning [14, 15].

To model the explosion of THF using the TNT equivalence method, the chemical energy of THF must be converted into an equivalent mass of TNT.

The equivalent mass of TNT (W_{TNT}) is calculated using the following equation:

$$W_{TNT} = \frac{\eta . m . \Delta H_C}{E_{TNT}} \tag{1}$$

where,

W_{TNT}: Equivalent mass of TNT (kg)

η: Explosion efficiency factor (dimensionless)

m: Mass of the THF involved in the explosion (kg)

ΔH_C: Heat of combustion of THF (kJ/kg)

E_{TNT}: Specific energy of TNT (standardized at 4,184 kJ/kg)

The explosion damage radius can be determined using Eq. (2) [16].

$$R1 = 0.396 . W_{TNT}^{\frac{1}{3}} . exp(3.503 - 0.72 ln\Delta P + 0.039(ln\Delta P)^2) \tag{2}$$

where, $R1$ is the explosion damage radius (m) and ΔP is the overpressure (kPa). The effects of over-pressure are presented in Table 4.

The minor injury radius $R2$ and death radius $R3$ and can be calculated using Eqs. (3) and (4) [16, 17].

$$\Delta P = 0.137 . [\frac{R_2}{\left(\frac{E}{p_0}\right)^{1/3}}]^{-3} + 0.119 . [\frac{R_2}{\left(\frac{E}{p_0}\right)^{1/3}}]^{-2} + 0.269 . [\frac{R_2}{\left(\frac{E}{p_0}\right)^{1/3}}]^{-1} \tag{3}$$

$$R3 = 13.6 . (\frac{W_{TNT}}{1{,}000})^{0.37} \tag{4}$$

$$E = W_{TNT} . Q_{TNT} \tag{5}$$

where, p_0 is atmospheric pressure (101 kPa).

Scenario 2—Thermal radiation from pool fire [18]

This simulation explores the consequences of an immediate ignition of the liquid spill. The released THF forms a puddle on the concrete substrate, which acts as the fuel source for a sustained pool fire. The model calculates the thermal radiation flux based on a flame height and a burn duration.

Scenario 3—BLEVE [19]

The most catastrophic scenario involves the sudden rupture of the tank due to external heat or structural failure, resulting in a BLEVE. The study models both a 50% and a 100% mass involvement.

Table 4. Overpressure levels and corresponding damage effects with blast radii ($R1$, $R2$, $R3$)

ΔP (kPa)	Explosion Effect	$R1$ (m)	$R2$ (m)	$R3$ (m)
1.04	Glass window damage	48,016.77	7.74	4.59
2.07	10% of the glass is broken	29,862.02	5.09	
3.45	Windows are damaged and the building structure is less damaged	21,498.70	3.73	
6.90	Parts of the structure are damaged	14,220.15	2.47	
13.80	Parts of walls and roofs collapsed	9,764.95	1.63	
16.56	Eardrum ruptures	8,900.97	1.48	
17.25	Critical illnesses	8,721.34	1.45	
20.70	Fracture of steel structure buildings	7,974.95	1.31	
34.50	Fracture of wood structure buildings	6,293.05	1.01	
69.00	Almost all buildings collapsed, and the lungs of personnel bleed	4,714.26	0.72	
138.00	Direct shockwaves are 100% fatal	3,666.39	0.52	

Scenario 4—BLEVE formation for road chemical tanker containing tetrahydrofuran [19]

THF is typically transported using specialized tank vehicles designed in accordance with the provisions of the ADR. In terms of capacity, road chemical tankers used for THF transportation generally have a typical volume ranging between 20 and 30 m³, and they may be designed either as single-compartment tanks or multi-compartment configurations, depending on operational requirements and distribution logistics.

In Kocaeli, Türkiye, which hosts numerous industrial facilities and port-related logistics activities, the road transportation of hazardous chemicals constitutes an important operational activity as well as a potential safety risk. In a hypothetical scenario, a road tanker with an approximate capacity of 24 m³ is assumed to be transporting the THF. The tanker is considered to be filled to approximately 80% of its total capacity and operating in compliance with the provisions of the ADR. While travelling along an industrial roadway characterized by heavy traffic, the tanker becomes involved in a multi-vehicle traffic accident. As a result of the collision, the tanker overturns and sustains mechanical damage to the outer shell of the tank. Simultaneously, fuel leaking from another vehicle involved in the accident ignites, initiating a fire in the immediate vicinity of the tanker. Prolonged exposure of the tanker to high temperatures generated by the surrounding fire causes a rapid increase in the temperature of the THF contained within the tank, which in turn leads to a significant rise in the internal vapor pressure. The upper portion of the tank wall, particularly the section located above the liquid level, is directly exposed to the flames and therefore experiences accelerated thermal weakening. As the temperature of the metal structure increases, its mechanical strength decreases progressively. If the fire continues and the tank is not sufficiently cooled or depressurized, the structural integrity of the tank may deteriorate to a critical level, resulting in sudden rupture. At this stage, the pressurized liquid inside the tank undergoes instantaneous flashing and rapid vapor expansion. This sudden phase transition and expansion may ultimately lead to a BLEVE, generating a violent explosion accompanied by the rapid.

3. RESULTS

3.1 Scenario 1—Passive dispersion (toxic vapor cloud of tetrahydrofuran)

This study investigates the consequences of a loss-of-containment event involving THF, a highly volatile and flammable cyclic ether extensively utilized as an industrial solvent and chemical intermediate. Given its low boiling point and significant vapor pressure, an accidental discharge of THF poses simultaneous toxicological and flammability hazards to industrial facilities and surrounding environments. Utilizing the ALOHA dispersion modelling software, this assessment simulates the atmospheric transport of a THF vapor cloud. The analysis incorporates site-specific meteorological conditions and storage configurations—specifically a vertical cylindrical tank—to delineate threat zones based on emergency response planning guidelines (ERPG) and thermal radiation thresholds [20]. By evaluating both the sustained evaporation from a liquid puddle and catastrophic tank failure modes, this research provides a deterministic framework for establishing emergency exclusion zones and enhancing QRA protocols for VOC storage units.

This scenario focuses on THF a highly volatile cyclic ether, stored in a vertical cylindrical tank/ storage vessel. The scenario models a catastrophic loss of containment through a 10-cm circular opening located at the bottom of the tank. Due to the position of the breach and the liquid state of the contents, the initial release is characterized by a high-velocity liquid-phase discharge rather than a gaseous leak. Upon contact with the concrete substrate, the released THF forms a spreading liquid puddle, which, driven by the chemical's high vapor pressure, acts as a continuous source for a toxic vapor cloud [21, 22].

In this study, the accidental discharge of THF was simulated as a liquid-phase release, resulting in a total discharge mass of 145 kg. The emission event spanned a duration of 36 min, maintaining a maximum average sustained release rate of 4.17 kg/min (Figure 1). Following the loss of containment, the liquid THF formed a spreading puddle on a concrete substrate, reaching a maximum diameter of 6.4 m. To ensure conservative estimation in the evaporation modelling, the ground temperature was assumed to be in thermal equilibrium with the ambient air.

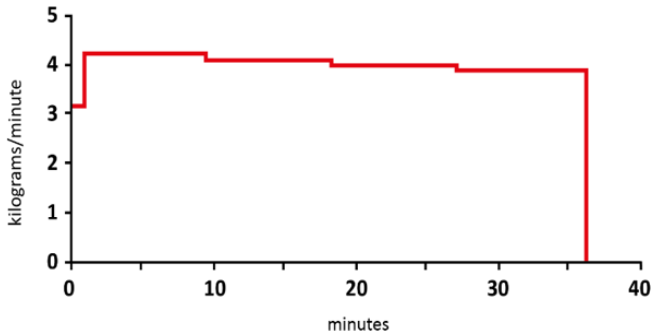

Figure 1. Evaporation rate of tetrahydrofuran (THF)

Utilizing the ALOHA modelling framework, this analysis simulates the atmospheric dispersion of the resulting plume as

it is transported downwind. The physical properties of the release—specifically the high discharge rate through a 10 cm orifice—ensure the formation of a sustained toxic plume. This assessment delineates the spatial extent of the vapor cloud against ERPG, defining critical safety perimeters where concentration levels may pose acute inhalation hazards to personnel.

The dispersion modelling results delineate the spatial distribution of the THF plume in relation to established ERPG thresholds. According to the simulation, the plume reaches the ERPG-1 level (100 ppm), which defines the area in which individuals may detect a distinct odour or experience mild, transient health effects that do not compromise their ability to undertake protective actions. In contrast, the higher toxicological thresholds ERPG-2 (500 ppm) and ERPG-3 (5000 ppm) are not exceeded within the modelled domain. Under the specified atmospheric conditions and release characteristics, including a sustained evaporation rate of 4.17 kg/min, this indicates that THF vapour concentrations remain below levels associated with irreversible health effects or life-threatening consequences.

Based on these results, and strictly under the assumption that no ignition, fire, or explosion occurs during the dispersion process, the primary toxicological impact may be considered limited to sensory irritation and odour perception within the ERPG-1 contour. In this context, the absence of exceedance of ERPG-2 and ERPG-3 supports the interpretation that acute severe toxic effects are not expected under the modelled conditions. However, this interpretation is valid only within the explicitly stated assumption of non-ignition conditions. It is important to emphasize that this assumption applies exclusively to the toxicological assessment framework. The flammable nature of the vapour cloud introduces an additional and independent hazard category related to ignition, fire, and explosion potential, which is not captured by toxic dispersion modelling alone. Therefore, limiting the analysis solely to toxic exposure outcomes would not provide a comprehensive risk characterization. When this distinction is clearly acknowledged, the logical consistency of the toxic risk interpretation is maintained while avoiding underestimation of the overall hazard. Assuming no ignition and no fire/explosion happens, then the direct toxic risk to people is mainly sensory irritation. Consequently, a complete process safety evaluation requires that toxic dispersion effects and flammability-related consequences be assessed separately but within an integrated risk assessment framework, ensuring that both exposure pathways are appropriately addressed.

The 10 cm hole diameter was selected as a conservative worst-case release condition rather than a routine operational leak. Smaller openings, such as 1 cm or 5 cm, would produce lower release rates and shorter hazard distances; however, the selected bounding case supports emergency planning by estimating the upper range of credible consequences. In this context, the 10 cm hole diameter considered in this study was intentionally selected to represent a conservative worst-case release scenario rather than a typical operational leak. In hazard identification, consequence analysis, and emergency management studies, the use of worst-case assumptions is a widely accepted methodological approach for evaluating the upper bounds of potential accident impacts. Such scenarios are particularly important in process safety and disaster management because they allow decision-makers to assess whether existing emergency response capacities, evacuation procedures, safety barriers, and land-use planning measures remain effective under severe but credible failure conditions.

From an emergency management perspective, worst-case scenario modelling serves as a precautionary framework aimed at minimizing the potential consequences of low-probability but high-impact events. Although incidents involving large tank-bottom breaches are relatively uncommon in routine industrial operations, historical industrial accidents have demonstrated that catastrophic failures can occur due to corrosion, mechanical damage, material fatigue, operational errors, external impacts, or cascading accident sequences. Therefore, analysing a severe release case provides valuable insight into the maximum possible hazard distances, thermal radiation effects, toxic dispersion zones, or overpressure impacts that may arise during a major accident.

The resulting toxic plume footprint, as illustrated in the dispersion model, indicates that the concentration exceeding the ERPG-1 threshold (100 ppm) extends 98 m downwind. This zone represents the area where individuals may experience mild, transient health effects or a noticeable odor. Notably, the higher severity thresholds, ERPG-2 (500 ppm) and ERPG-3 (5000 ppm), were not reached under the defined source strength and atmospheric conditions (Figure 2). The dispersion analysis of the THF release reveals critical findings regarding the immediate vicinity of the source. While the ERPG-1 boundary was clearly defined, the high-severity threat zones- specifically the red zone (ERPG-3, >5000 ppm) and the orange zone (ERPG-2, >500 ppm)—were not explicitly drawn in the model output. Technically, the ERPG-3 threshold was estimated to occur within a distance of less than 10 m, while the ERPG-2 threshold was confined to within 42 m of the release point. However, these zones were omitted from the visual representation due to near-field patchiness, a phenomenon where localized turbulence and incomplete mixing at short distances make standard dispersion predictions unreliable. Consequently, while these hazardous concentrations exist in close proximity to the spill, the model acknowledges that deterministic plume boundaries cannot be accurately mapped in the immediate near-field region.

In addition to the toxicological assessment, the model evaluated the flammable area of the vapor cloud based on Lower Explosive Limit (LEL) thresholds [23]. The analysis focused on two critical concentration levels: the 60% LEL (12,000 ppm) and the 10% LEL (2,000 ppm) zones. However, similar to the high-severity toxic zones, the flammable threat zones were not explicitly drawn in the model output. This omission is attributed to near-field patchiness, where the localized variability in vapor concentration at short distances from the release point prevents a reliable deterministic prediction of the flammable cloud's boundaries. Consequently, while a fire or explosion hazard exists in the immediate vicinity of the THF spill, the model indicates that the dispersion behavior within this near-field region is too turbulent for precise spatial mapping. Regarding the fire and explosion hazards of the release, the model identified two critical flammability zones based on vapor concentration. The high-risk flammable zone (red), defined by concentrations exceeding 60% LEL (12,000 ppm), was estimated to occur within a very localized radius of less than 10 m from the source. Additionally, the Lower-risk flammable zone (yellow), which represents the 10% LEL (2,000 ppm) threshold commonly used as a safety buffer for ignition source control, was found to extend to approximately 17 m. Despite these calculated distances, these threat zones were not

explicitly drawn in the model output due to near-field patchiness, a condition where localized turbulence near the release point makes deterministic dispersion predictions unreliable at short ranges.

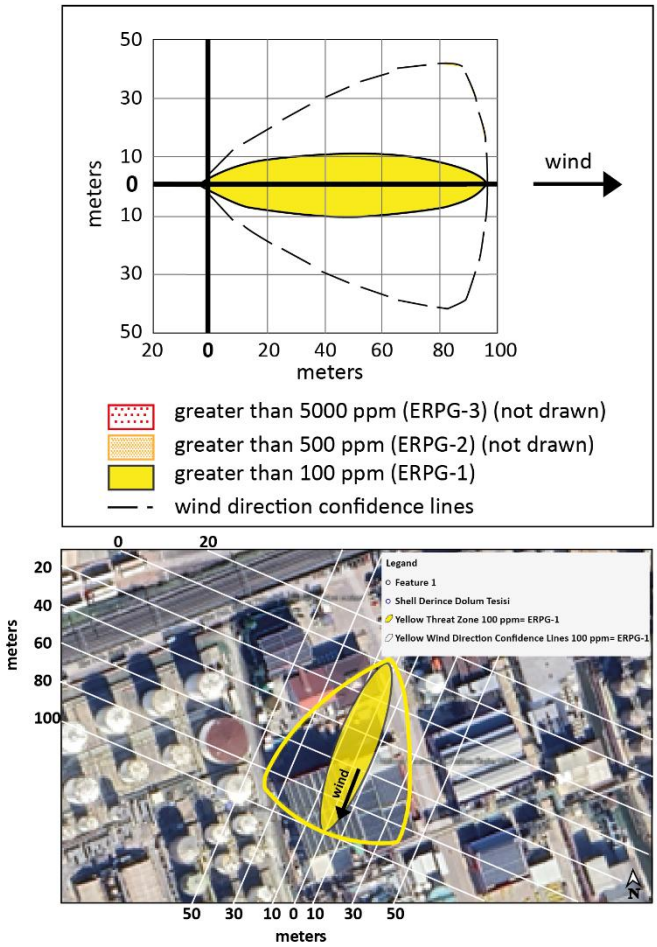

Figure 2. Toxic threat zones of tetrahydrofuran (THF)

Similar to the high-severity toxic zones, these flammable threat zones were not explicitly mapped in the model output. This is due to near-field patchiness, where localized turbulence and incomplete mixing near the release point result in concentration fluctuations that standard dispersion models cannot deterministically predict. Consequently, while an ignition hazard exists within the first 17 m, the boundaries of this risk area are considered unstable. A significant finding of the analysis is the absence of a VCE risk under the specified conditions. The simulation indicates that no part of the THF cloud exceeds the LEL at any point in time, assuming a non-congested environment. Therefore, the model predicts no overpressure or blast force effects, as the vapor concentration remains below the threshold required to sustain a stoichiometric explosion. This suggests that the primary hazard of the release is confined to localized fire risk (flash fire) and toxic inhalation rather than a catastrophic pressure event.

3.1.1 Investigation of explosion damage, death and minor injury radius for vapor cloud explosion of tetrahydrofuran using TNT equivalence formula

The provided dataset delineates the quantitative correlation between peak overpressure (ΔP) and the corresponding vulnerability thresholds for both structural integrity and human physiology. From a fluid dynamics perspective, the data illustrates the attenuation of shock waves as they propagate through the atmosphere; as the explosion damage radius ($R1$) increases, the overpressure decays following an inverse power-law relationship, typical of spherical wave expansion. The extreme range observed for glass damage (48,017.77 at 1.04 kPa) underscores the high susceptibility of brittle materials to low-energy impulse loads, marking the primary damage zone in industrial accident modelling.

In terms of structural mechanics, the transition from non-structural damage (glass breakage) to primary structural failure (fracture of steel and wood frames) occurs within the 20.70 to 34.50 kPa range. This indicates the point where the dynamic load imposed by the blast wave exceeds the yield strength of standardized construction materials. Furthermore, the biological impact data highlights a critical hierarchy of injury: auditory trauma (eardrum rupture) manifests at relatively moderate pressures (16.56 kPa), whereas visceral trauma, specifically pulmonary haemorrhage, requires significantly higher energy densities (69.00 kPa). The 138.00 kPa threshold represents the lethality limit, where the magnitude of the pressure gradient causes instantaneous and irreversible barotrauma. Consequently, these values serve as essential parameters for QRA and the establishment of safety buffer zones in urban planning and hazardous material storage.

When these two perspectives are integrated, it becomes clear that the human lethality zone is significantly smaller ($R1$ = 3,666.39 m) than the structural damage zone (48,016.77 m). This disparity is a cornerstone of emergency response planning, suggesting that while the immediate vicinity of a blast requires search-and-rescue for survivors, the vast majority of the affected area will require glass-hazard mitigation and civil engineering assessments.

The QRA derived from this dataset establishes a multi-tiered safety hierarchy, where the spatial coordinates ($R1$, $R2$, and $R3$) define the extent of the hazard zones based on specific damage probabilities [24]. At the core of this assessment is the inner lethal zone, where the $R3$ values correspond to a high-fatality probit function; in this region, the overpressure exceeding 138 kPa ensures that the primary shockwave interaction is 100% fatal, necessitating an absolute exclusion perimeter for unprotected personnel. Moving outward, the $R2$ values delineate the structural instability zone, where the focus shifts from direct barotrauma to secondary hazards, such as the collapse of steel and timber frames. The rapid decay of pressure relative to the $R2$ distance suggests that structural hardening is only effective within a specific, narrow range before the energy density falls below the threshold of total mechanical failure.

On a macro-geographical scale, the $R1$ values represent the extensive impact radius, which is critical for urban planning and emergency response mobilization. The vast discrepancy between the 138 kPa radius (3,666.39 m) and the 1.04 kPa glass-damage radius (48,016.77 m) illustrates that the casualty-producing area- driven by flying debris and shattered glass-is significantly larger than the area of direct blast lethality. Consequently, a robust QRA based on these figures prioritizes the mitigation of "glass rain" and non-structural debris in the outer contours, while reserving heavy-duty protective infrastructure for the inner $R2$ and $R3$ perimeters. This spatial stratification allows risk managers to quantify the societal risk and establish mandatory standoff distances that prevent a localized industrial failure from escalating into a regional humanitarian catastrophe [24].

The data represents a typical blast wave attenuation profile, where the peak static overpressure is evaluated against three distinct distance parameters. In blast physics, these values often correspond to different safety perimeters or theoretical models of wave propagation.

The overpressure results in Table 4 should be interpreted as screening-level TNT-equivalence outputs. The large *R*1 value at 1.04 kPa (48,016.77 m) reflects the very low threshold for glass damage and the far-field extrapolation behaviour of simplified blast-scaling equations. This value should not be read as an expected real-world damage distance, because terrain, building shielding, atmospheric attenuation, and energy dissipation would substantially reduce actual blast propagation. Therefore, the 48 km value is retained only as a conservative theoretical upper-bound indicator for comparative hazard assessment, while the minor-injury and death radii are the more relevant near-field safety indicators. In addition, it can be safely mentioned that this is a theoretical extrapolation and wouldn't actually happen.

3.2 Scenario 2—Thermal radiation from pool fire of tetrahydrofuran

An analysis of the time-dependent discharge rate for the THF leak reveals a dual-phase emission characteristic. Initially, the discharge rate begins at approximately 80 kg/min. Within the first 0.4 min, the rate rapidly escalates to a peak of 100 kg/min, maintaining this steady-state condition throughout the total 1.5-minute primary discharge duration (Figure 3). This transition from a high-intensity short-term discharge to a lower-intensity sustained evaporation phase is critical for defining both the immediate flammability risks and the long-term toxicological footprint of the spill.

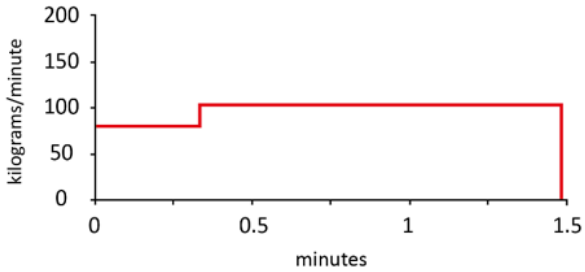

Figure 3. Burn rate of tetrahydrofuran (THF)

Figure 3 describing the emission dynamics is directly linked to the thermal radiation of a pool fire through the concepts of fuel supply and burn duration. In a pool fire scenario, the thermal energy released is a function of the surface area of the liquid and the rate at which that liquid is supplied or evaporated. The transition from a high-intensity discharge to a sustained evaporation phase dictates the lifecycle and intensity of the thermal hazard. The initial high-intensity discharge (peaking at 100 kg/min) determines how quickly the THF spreads across the concrete substrate. Since the discharge rate far exceeds the burning rate of the liquid, a large puddle form rapidly. The sustained emission rate maintains the source term for the fire. In a pool fire, the heat of combustion interacts with the evaporation rate; the more fuel is available at the surface, the more sustained the flame length. In summary, the emission profile acts as the source term for the fire. The initial rapid leak creates the physical footprint, while the cumulative mass and evaporation rate determine how long the intense thermal radiation will persist and how far its lethal red zone will extend.

In the event of ignition, the THF puddle would result in a pool fire, generating significant thermal radiation levels across three distinct threat zones. The red zone, characterized by a thermal radiation intensity of 10.0 kW/m², is estimated to extend up to 14 m from the center of the spill, a level at which exposure is considered potentially lethal within 60 seconds. Beyond this, the injury threat zone (orange) reaches 19 m with a radiation intensity of 5.0 kW/m², which is sufficient to cause second-degree burns within the same 60-second timeframe. Finally, the pain threshold zone (yellow) extends to a distance of 27 m at an intensity of 2.0 kW/m², causing physical pain to exposed individuals within 60 seconds (Figure 4).

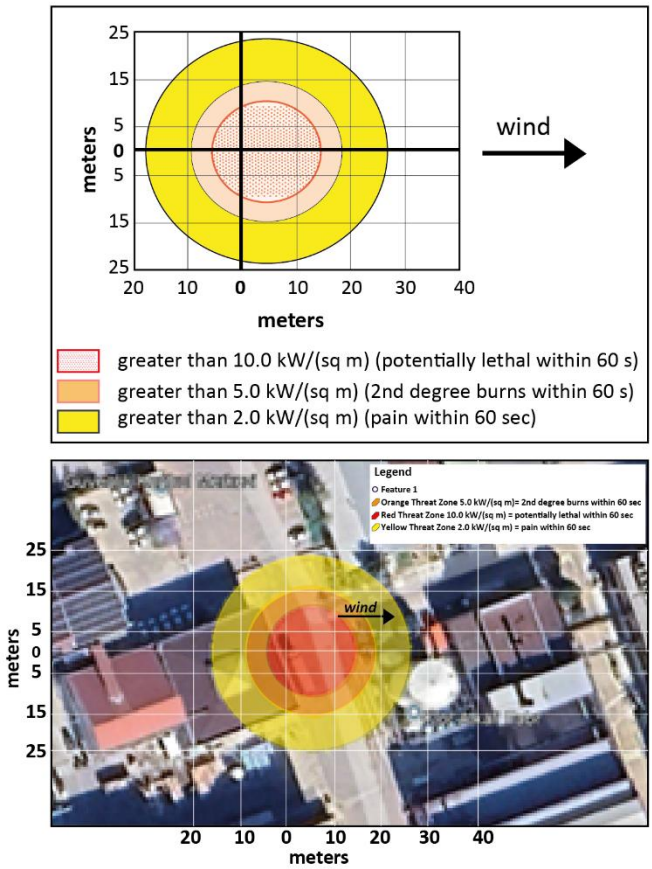

Figure 4. Thermal radiation from pool fire of tetrahydrofuran (THF)

These distances are critical for defining the immediate physical danger radius, which is more compact than the 100 m toxicological footprint but requires more urgent physical evacuation due to the rapid onset of thermal injuries. These findings indicate that while the toxic plume (ERPG-1) extends significantly further (100 m), the immediate physical danger from a fire-including lethality and severe burns-is concentrated within a 27 m radius of the release point. This highlights the critical importance of maintaining a strict exclusion zone for all non-essential personnel and ignition sources in the immediate vicinity of the concrete substrate during the initial 36 minutes of the release.

3.3 Scenario 3—Boiling liquid expanding vapor explosion of tetrahydrofuran

The storage system comprises a vertical cylindrical tank with a total volume of 202 liters, containing 144 kg of liquid

THF. A catastrophic failure was modelled as a BLEVE scenario where 50% of the tank mass participates in the immediate fireball [25]. This event results in the formation of a fireball with a 24 m diameter and a brief but high-intensity burn duration of 3 s, representing an extreme thermal flux event capable of causing immediate lethality within its radius. Following the initial explosion, the residual liquid contributes to a 5 m diameter pool fire with a burn duration of 54 seconds and a flame length of 10 m. This secondary phase provides a sustained thermal load that poses a significant risk of domino effects, such as the thermal weakening of adjacent structures or the ignition of nearby flammable materials on the concrete substrate.

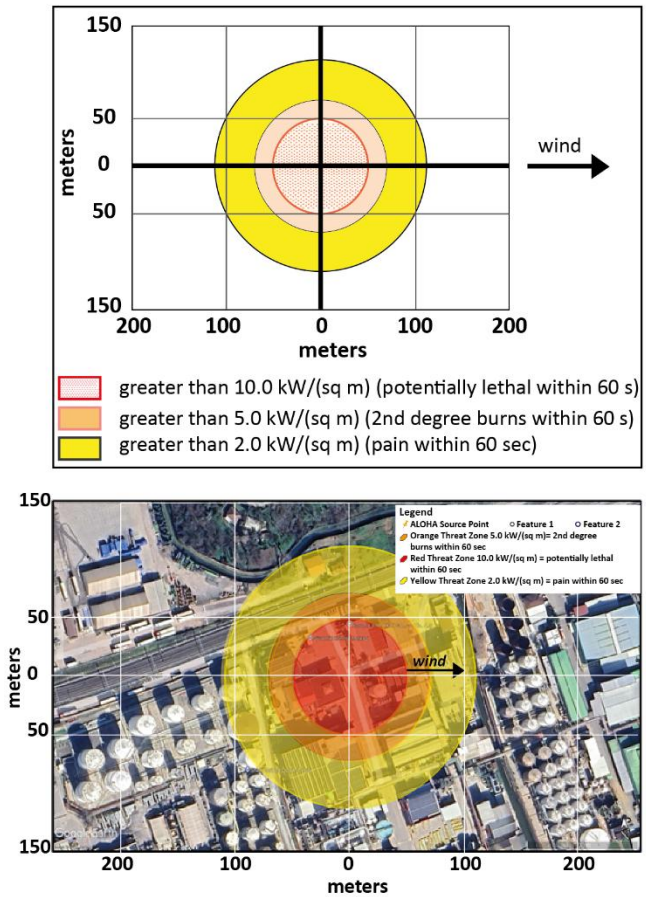

Figure 5. Thermal radiation from fireball (50% of tank mass participates in the fireball) of tetrahydrofuran (THF)

The thermal radiation impacts resulting from a 50% mass fraction BLEVE involving THF establish a tiered hierarchy of hazard zones based on the magnitude of heat flux. The potential lethality zone (red), defined by a critical threshold of 10.0 kW/m², extends to a radius of 50 m; while this intensity typically causes fatalities within a 60-second exposure, the concentrated energy release of a 3-second fireball suggests that unprotected personnel within this perimeter face nearly instantaneous, life-threatening injuries. Beyond this core, the severe injury zone (orange) reaches 71 m, where a radiation intensity of 5.0 kW/m² is sufficient to induce second-degree burns within a one-minute timeframe, marking a vital boundary for emergency responder safety and the demarcation of exclusion zones. Finally, the pain threshold and low-risk zone (yellow) serve as the outermost hazard perimeter, extending to 112 m at a flux of 2.0 kW/m². At this distance, the primary risk is limited to the onset of physical pain, providing a comprehensive spatial framework for disaster management and structural setback planning. Comparing these results to the pool fire scenario (where the pain threshold was limited to 27 m) and the toxic plume (ERPG-1 at 100 m), the BLEVE event clearly represents the maximum credible hazard distance for the facility [25-27]. The thermal impact of the explosion surpasses the toxic footprint, necessitating a primary safety exclusion radius of at least 112 m to protect against all immediate physical hazards (Figure 5).

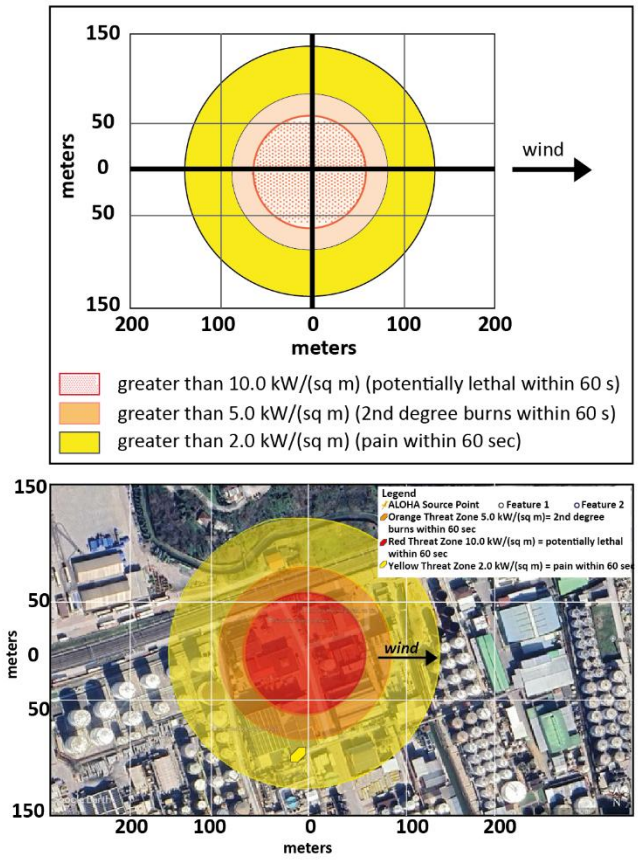

Figure 6. Thermal radiation from fireball (100% of tank mass participates in the fireball) of tetrahydrofuran (THF)

The following analysis evaluates the catastrophic consequences of a 100% mass fraction BLEVE involving the THF storage unit [25]. In this worst-case scenario, the model assumes a total loss of containment where 100% of the tank mass participates in the resulting fireball. In a worst-case scenario, the fireball geometry and Intensity are significantly amplified, resulting in a fireball with a 30 m diameter. This represents a substantial expansion of the immediate physical flame footprint compared to partial failure models. The associated temporal hazard is characterized by an intense, brief duration of 3 seconds; this extreme concentration of energy release generates a massive thermal flux that poses a near-instantaneous threat of lethality and severe structural damage to any assets within or adjacent to the 30 m radius. Furthermore, the significance of the tank fill level is paramount; the high liquid-to-vapor ratio ensures that the energy release is driven by the rapid phase transition and combustion of the liquid phase, yielding a much more potent thermal radiation threat than a purely vapor-driven explosion. In summary, the 100% BLEVE represents the absolute maximum credible fire hazard for this specific storage configuration. The resulting 30 m fireball defines the total

destruction zone, where secondary fires and structural failures are virtually guaranteed. In a catastrophic 100% mass involvement scenario, the thermal hazard perimeters expand significantly to define three critical zones of impact. The potential lethality zone (red), governed by a 10.0 kW/m² threshold, extends to a radius of 62 m; although the fireball persists for only 3 seconds, the sheer magnitude of the instantaneous heat flux within this area is sufficient to inflict fatal thermal trauma on unprotected personnel. Beyond this, the severe injury zone (orange) reaches 89 m, where a radiation intensity of 5.0 kW/m² causes second-degree burns within a 60-second window, marking the definitive safety boundary for emergency response operations. The final perimeter, the pain threshold zone (yellow), extends to 139 m at a flux of 2.0 kW/m², representing the maximum distance at which the explosion's thermal effects are physically perceivable as pain (Figure 6).

The transition from a 50% mass involvement to 100% mass involvement increases the pain threshold distance from 112 m to 139 m, and the lethality radius from 50 m to 62 m. Consequently, the 139 m radius now defines the primary life safety exclusion zone for the facility, as it exceeds the 100 m toxicological footprint (ERPG-1) and the 17 m flammability buffer. This 139 m zone should be the basis for all catastrophic emergency response planning and structural setback requirements.

3.4 Scenario 4—Boiling liquid expanding vapor explosion formation for road chemical tanker containing tetrahydrofuran

Following the road chemical tanker rupture and the rapid depressurization of the contained THF during the surface transportation, the event is assumed to develop into a BLEVE, accompanied by the formation of a large fireball. The tanker is assumed to have a total capacity of approximately 24 m³, while the liquid volume inside the road chemical tanker is estimated to be 19 m³, corresponding to an 80% filling ratio during transportation.

Such a fireball can generate severe levels of thermal radiation capable of causing significant damage to nearby vehicles, infrastructure, and industrial facilities, as well as posing a serious risk to human life within the affected area. Consequently, these parameters provide a basis for evaluating the potential impact zones and emergency response requirements associated with a BLEVE event during hazardous material transportation [28].

The total chemical mass in the road chemical tanker is 17,144 kg, with the tanker filled to approximately 80% of its capacity. In the event of a BLEVE, it is assumed that 50% of the tanker mass participates in the fireball formation, resulting in a fireball with an estimated diameter of 119 m and a burn duration of 9 s. Under a more severe scenario, 100% of the tanker mass may contribute to the fireball, producing a larger fireball with a diameter of 150 m and a burn duration of 10 s. Concurrently, the scenario predicts the development of a pool fire with a diameter of 51 meters and a burn duration of 54 s, producing a maximum flame length of approximately 55 m.

In the first scenario, 50% of the road chemical tanker mass is involved in the fireball. The thermal radiation threat zones for this scenario indicate that the red zone (10 kW/m², potentially lethal within 60 seconds) extends 230 m, the orange zone (5 kW/m², capable of causing 2nd degree burns within 60 seconds) extends 326 m, and the yellow zone (2 kW/m², capable of producing pain within 60 seconds) reaches 511 m (Figure 7). In the second, more severe scenario, 100% of the tanker mass contributes to the fireball. The corresponding thermal radiation threat zones expand significantly, with the red zone extending to 286 meters, the orange zone to 407 meters, and the yellow zone to 637 meters. Comparatively, increasing the fraction of the tanker mass involved in the BLEVE from 50% to 100% leads to a substantial expansion of the thermal radiation threat zones. Specifically, the red zone, corresponding to a thermal intensity of 10 kW/m² and representing potentially lethal exposure within 60 seconds, increases by approximately 26%, from 230 meters to 286 meters. The orange zone, associated with 5 kW/m² and capable of causing second-degree burns within the same timeframe, expands by about 25%, from 326 meters to 407 meters. Similarly, the yellow zone, defined by 2 kW/m² and representing conditions sufficient to produce pain within 60 seconds, grows by roughly 25%, extending from 511 meters to 637 meters. These proportional increases underscore the critical influence of the participating road chemical tanker mass on the spatial extent of thermal hazards in BLEVE events (Figure 7).

Chapter 1: Comparison of Scenarios 3 and 4 shows that the road-tanker BLEVE is the bounding case in terms of spatial impact. For full mass involvement, the storage-tank BLEVE reaches 139 m at the 2.0 kW/m² threshold, whereas the road-tanker BLEVE reaches 637 m. This difference is mainly driven by the larger transported inventory and vessel configuration, which produce a larger fireball and wider thermal radiation footprint.

Chapter 2: From an emergency-response perspective, the road-tanker BLEVE requires a wider initial isolation perimeter, rapid traffic control and evacuation, and defensive response operations until the fireball phase has passed. Accordingly, the 637 m road-tanker result should be treated as the primary worst-case planning distance for transport incidents, while the storage-tank BLEVE distances support facility-scale planning. When compared across scenarios, it becomes evident that the road tanker BLEVE represents the dominant hazard case in terms of spatial impact, exceeding both the storage tank BLEVE and the toxic dispersion footprint. In particular, even the most conservative toxic plume estimate (ERPG-1 at 100 m) remains well within the thermal radiation zones of the road tanker fireball, confirming that thermal effects govern the maximum credible hazard distance for this system. Accordingly, these findings collectively suggest that emergency planning for road transportation accidents should prioritize thermal exclusion distances derived from BLEVE scenarios, as they define the outermost and most restrictive safety perimeters. The results therefore provide a coherent hierarchy of risk, where increasing mass involvement systematically amplifies thermal hazard zones and establishes the road tanker BLEVE as the bounding case for emergency response planning. In addition, from an emergency response perspective, the results obtained for the BLEVE scenarios have important implications for operational planning, particularly in the establishment of exclusion zones and the prioritization of response strategies. The predicted thermal radiation distances indicate that, especially in the case of road tanker involvement, hazardous conditions may extend over several hundred meters, reaching up to the outer pain threshold zone. This suggests that first responders would be unable to safely approach the incident site during the initial phase of a BLEVE event without

exposure to potentially injurious or lethal thermal radiation. Accordingly, the outermost thermal radiation boundary (2 kW/m²), corresponding to the pain threshold, should be considered as a minimum guideline for the initial establishment of safety perimeters and scene isolation. Within this zone, rapid evacuation of the surrounding population and restriction of access are essential to prevent secondary casualties. The intermediate zones (5 kW/m² and 10 kW/m²), associated with severe injury and lethality thresholds, respectively, further define operationally critical regions where direct intervention would not be feasible during the fireball duration due to the extremely short exposure times and high heat flux levels characteristic of BLEVE events.

Chapter 3: The comparative analysis between storage tank and road tanker scenarios further indicates that transportation-related BLEVE events may generate significantly larger thermal hazard footprints, despite involving similar substances [29]. This finding underscores the need for more conservative emergency planning assumptions in road transport contexts, where rupture conditions and rapid depressurization may result in more extensive fireball development. Overall, the results highlight that emergency response strategies for BLEVE incidents should prioritize rapid area evacuation, early establishment of large exclusion zones, and defensive rather than offensive firefighting tactics during the initial fireball phase. These findings emphasize that effective management of BLEVE events relies primarily on exposure prevention rather than direct intervention, particularly in scenarios involving hazardous material transportation.

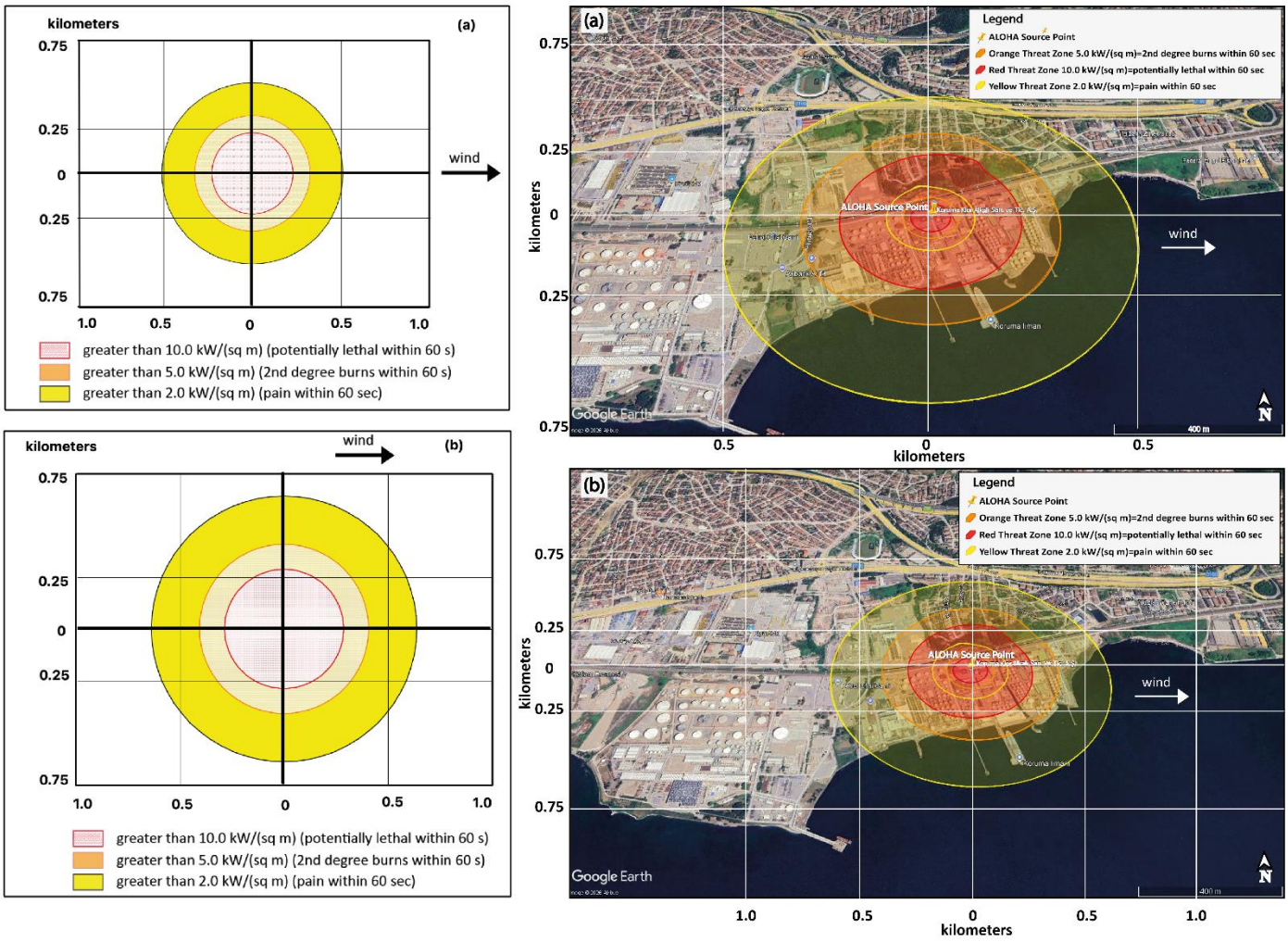

Figure 7. Thermal radiation from fireball ((a) 50% (b) 100% of road chemical tanker mass participates in the fireball) of tetrahydrofuran (THF)

4. DISCUSSION

The four modelled accident scenarios—non-ignited toxic dispersion, pool fire, storage-tank BLEVE, and road-tanker BLEVE—represent progressively escalating consequence pathways associated with the accidental release of THF. Each scenario produces a distinct spatial and temporal hazard footprint. The toxic dispersion scenario is characterized by sustained vapor generation resulting from liquid evaporation following loss of containment. The ERPG-1 threshold extends up to 98 m downwind, while higher ERPG thresholds remain confined to the near-field region. This scenario produces the widest spatial footprint in terms of toxic exposure duration but does not generate significant thermal or overpressure effects. In contrast, the pool fire scenario generates a more spatially compact hazard footprint, with thermal radiation distances limited to 27 m at the lowest reported radiation threshold. The temporal characteristics of the pool fire differ from the toxic dispersion scenario, as the fire hazard is concentrated over a shorter time interval but involves higher instantaneous energy

release.

The storage-tank BLEVE scenarios produce larger thermal footprints than the toxic dispersion and pool-fire scenarios, with 2.0 kW/m² distances of 112 m and 139 m for 50% and 100% mass involvement, respectively. The road-tanker BLEVE represents the maximum spatial hazard, extending to 511 m and 637 m for 50% and 100% mass involvement. These differences show that inventory scale and vessel configuration strongly govern emergency-planning distances.

4.1 Relative dominance of hazards

The reported results indicate that different hazard types dominate under different accident conditions. In the non-ignited release scenario, toxic exposure represents the primary hazard, as evidenced by the spatial extent of the ERPG-1 threshold relative to other modelled effects. Although flammability thresholds are present in the near-field region, the dispersion results show no development of VCE effects under the defined conditions.

In the pool fire scenario, thermal radiation becomes the dominant hazard, replacing toxic exposure as the primary concern within a limited spatial radius. The reported radiation contours demonstrate that the fire hazard is concentrated near the release point, with decreasing intensity at increasing distances. The duration of the pool fire and associated burn rates define the temporal persistence of this hazard [29, 30].

The BLEVE scenarios exhibit dominance of thermal radiation hazards over all other modelled effects. The fireball radiation distances exceed both the toxic dispersion footprint and the pool fire radiation distances. Although explosion overpressure effects are calculated using the TNT equivalence method, the dominant spatial hazard in BLEVE scenarios remains thermal radiation, as reflected in the reported radiation distances [31]. The short duration of the fireball distinguishes BLEVE events from sustained pool fire scenarios, while the spatial reach of thermal effects exceeds that of the other modelled hazards [32].

4.2 Implications for emergency planning and disaster risk reduction

The scenario-based results provide quantitative information that is directly applicable to emergency planning and DRR strategies. The toxic dispersion analysis defines exclusion zones relevant to early-stage response actions, including evacuation decisions, shelter-in-place measures, and the positioning of responders during non-ignited release events. In particular, the spatial extent of the ERPG-1 zone highlights the need for preparedness measures extending beyond the immediate vicinity of the release point [33, 34].

Similarly, the pool fire results contribute to emergency response planning in terms of ignition control, fire suppression operations, and responder safety. The calculated thermal radiation distances define zones within which direct exposure to hazardous thermal effects may occur during sustained combustion, thereby supporting the establishment of operational safety perimeters during firefighting activities.

The BLEVE scenarios provide critical input for worst-case emergency planning [35]. The resulting thermal radiation distances represent maximum credible hazard zones that are relevant for land-use planning, transport route design, and emergency preparedness strategies. Moreover, the distinction between partial and full mass involvement scenarios emphasizes the importance of accounting for variability in accident severity when developing response strategies. Collectively, these findings support a layered DRR framework that incorporates both frequent low-severity events and less frequent but high-consequence scenarios [36].

In addition, the study yields clearly defined quantitative impact distances, such as 98 m, 139 m, and 637 m, corresponding to different toxic and thermal threshold levels. However, the lack of an explicit linkage between these numerical results and their operational implications limits their direct usability in field-based emergency management. Therefore, associating the calculated hazard distances with structured emergency response zones would significantly enhance the practical relevance of the study. Specifically, the approximately 98 m ERPG-1 threshold can be interpreted as an early warning and public information zone, where the primary focus is on risk communication, public notification, and precautionary protective actions rather than evacuation. In contrast, the 139 m distance corresponding to the 2.0 kW/m² thermal radiation threshold in the BLEVE scenario may be defined as a mandatory evacuation zone, where immediate relocation of exposed populations is required due to the risk of harmful thermal effects. Finally, the maximum hazard distance of up to 637 m in the road tanker BLEVE case represents a primary exclusion zone under worst-case conditions. This boundary is critical for access control, traffic restriction, and the safe positioning of emergency command operations, ensuring that both responders and the public remain outside the area of potential direct impact during the initial phase of the incident.

It can be safely stated that the calculated impact distances should not be interpreted solely as physical consequence outputs, but rather as actionable decision-support parameters that can be directly integrated into emergency management frameworks such as the Incident Command System (ICS), evacuation planning, and land-use regulation strategies. In this context, the quantitative thresholds derived from the hazard analysis provide a structured basis for defining operational safety zones and supporting real-time decision-making during hazardous material incidents.

4.3 Comparison with similar studies

The results of this study are consistent with previously cited literature addressing VOC-related industrial and transport accidents, which emphasize the multi-hazard nature of such events [37, 38]. Prior studies referenced in the article highlight the importance of considering both toxic and physical hazards when evaluating chemical accident consequences. The spatial patterns observed in the toxic dispersion and thermal radiation results align with the general findings reported in earlier modelling-based assessments of VOC releases using atmospheric dispersion tools [10].

The application of ALOHA for consequence modelling is consistent with its documented use in emergency preparedness and industrial risk analysis [39]. The reported results reinforce the role of scenario-based modelling in supporting disaster management decision-making, particularly in regions with high concentrations of hazardous material transport and storage activities. By focusing on a specific chemical and storage configuration, the study complements existing literature by providing detailed, location-specific insights without extending beyond the scope defined in the original references.

4.4 Limitation of the study

The modelling approach incorporates several assumptions and conservative elements that influence the reported results. Meteorological conditions were held constant during each simulation, and ground temperature was assumed to be equal to ambient air temperature for evaporation modelling. Because wind speed, wind direction, humidity, and atmospheric stability can change over time, the reported plume and thermal distances should be interpreted as scenario-specific outputs rather than universal fixed boundaries. More stable atmospheric conditions or lower wind speeds could increase downwind toxic dispersion distances, while more unstable conditions could enhance mixing and reduce impact ranges. In this context, the use of a fixed meteorological condition (wind speed of 3 m/s and atmospheric stability class C) was intended to provide a representative and controlled basis for comparative analysis of the dispersion scenarios. However, it is acknowledged that atmospheric conditions are inherently variable and can significantly influence toxic dispersion behaviour. In particular, more stable atmospheric conditions (e.g., stability classes D–F) and lower wind speeds may reduce atmospheric mixing and lead to increased downwind travel distances of the toxic plume. Conversely, more unstable conditions may enhance dispersion and reduce impact ranges. Therefore, the presented results should be interpreted as scenario-specific outcomes, and the potential variability associated with changing meteorological conditions should be considered as an inherent limitation of the study.

Additional uncertainty arises from near-field patchiness and the simplified empirical models used for consequence estimation. Near-field turbulence limits the deterministic representation of hazard boundaries close to the release source.

Similarly, the TNT equivalence method is used only as a conservative screening approach; therefore, the 48 km glass-damage distance should be interpreted as a theoretical upper-bound extrapolation rather than an expected real-world damage radius. It can be safely mentioned that this is a theoretical extrapolation and wouldn't actually happen. In practice, terrain, building shielding, atmospheric attenuation, and energy dissipation would substantially reduce blast propagation.

Finally, the study is limited to consequence modelling and does not estimate accident frequency, probability, prevention-system performance, or human behavioural response. The results are therefore intended to support emergency planning, exclusion-zone definition, and DRR decisions under defined scenario assumptions, rather than to provide a full QRA.

5. CONCLUSIONS

This study conducted a consequence-based assessment of accidental THF release scenarios relevant to industrial storage and surface transport conditions in the Kocaeli–Izmit region of Türkiye. Using a deterministic modelling approach, the analysis focused on four representative accident scenarios: non-ignited liquid release leading to toxic vapor dispersion, pool fire following immediate ignition, storage-tank BLEVE, and road-tanker BLEVE with partial and full mass involvement. Atmospheric dispersion, thermal radiation, and explosion effects were modelled using the ALOHA 5.4.7 framework in combination with established empirical methods under site-specific meteorological and storage conditions. The study was explicitly limited to consequence modelling and did not address accident frequency, probability, or prevention measures.

The results demonstrated that each scenario produces a distinct hazard footprint in terms of spatial extent and dominant hazard type. In the non-ignited release scenario, toxic dispersion constituted the primary hazard, with the ERPG-1 concentration threshold extending up to 98 m downwind, while higher ERPG thresholds remained confined to the near-field region. Flammability zones based on LEL thresholds were limited to short distances from the release point, and no VCE overpressure effects were generated in the dispersion modelling output. Explosion overpressure distances calculated using the TNT equivalence method yielded extensive damage radii at low overpressure thresholds, with minor injury and death radii remaining confined to the near-field region. In the pool fire scenario, thermal radiation effects were spatially concentrated near the source, with radiation distances extending to 14 m at 10.0 kW/m², 19 m at 5.0 kW/m², and 27 m at 2.0 kW/m². The BLEVE scenarios produced the largest thermal radiation footprints among the modelled cases. For 50% mass involvement, thermal radiation distances reached 50 m, 71 m, and 112 m for the 10.0, 5.0, and 2.0 kW/m² thresholds, respectively, while full mass involvement increased these distances to 62 m, 89 m, and 139 m. For the road chemical tanker BLEVE scenarios, the extent of thermal radiation hazard zones increased significantly as the fraction of tanker mass involved grows. With 50% of the mass, potentially lethal zone reached 230 m, the 2nd-degree burn zone 326 m, and the pain zone 511 m. When 100% of the mass was involved, these distances expanded to 286 m, 407 m, and 637 m, respectively—an increase of approximately 25–26%. These results highlight the critical impact of the participating tanker mass on the spatial extent of thermal hazards.

These findings are directly relevant to DRR and emergency planning for facilities and transport operations involving THF. The quantified toxic dispersion distances support the definition of exclusion zones and response perimeters for non-ignited release scenarios, while the pool fire and BLEVE results provide spatial benchmarks for fire response, responder safety, and worst-case emergency planning. The differentiation between sustained hazards, such as toxic dispersion and pool fires, and short-duration, high-intensity hazards associated with BLEVE events highlights the importance of scenario-based planning that accounts for both spatial extent and temporal characteristics of chemical accidents. By providing consistent, scenario-specific consequence distances under defined conditions, this study contributes actionable information for emergency preparedness, land-use planning, and DRR strategies related to the storage and surface transport of VOCs.

REFERENCES

[1] Benouar, D., Benmokhtar, A. (2025). Risk governance for the implementation of the Sendai Framework for Disaster Risk Reduction in Algeria. International Journal of Disaster Risk Science, 16(1): 58-70. https://doi.org/10.1007/s13753-025-00619-4

[2] Lu, K., Chen, Y., Li, L., Zheng, Y., Wang, J., Pan, Y. (2026). Integrated design and performance validation of an advanced VOC and Paint mist recovery system for shipbuilding robotic spraying. Processes, 14(7): 1047.

https://doi.org/10.3390/pr14071047
[3] Ward, P.J., Buijs, S.L., Ciurean, R., Claassen, J.N., et al. (2026). Reducing risk together: Moving towards a more holistic approach to multi-hazard and multi-risk assessment and management. Natural Hazards and Earth System Sciences, 26(3): 1325-1345. https://doi.org/10.20858/sjsutst.2023.119.2
[4] Moriyama, T., Iwamoto, K., Sasaki, H., Sakiyama, H., Kanaizuka, K., Fujii, S. (2026). Concentration and crystallization of lithium chloride in tetrahydrofuran using laser-local heating and laser-induced microbubbles. Chemistry Letters, 55(3): upag032. https://doi.org/10.1093/chemle/upag032
[5] Liu, B., Zhan, L., Lu, H., Lu, X., Cai, W. (2022). Effect of the temperature and tetrahydrofuran (THF) concentration on THF hydrate formation in aqueous solution. Energy & Fuels, 36(18): 10642-10651. https://doi.org/10.1021/acs.energyfuels.1c03998
[6] Zhao, Y., Luan, T., Huang, J., Zhang, Y., Yang, G. (2025). Identification and quantification of risk factors for road transport of hazardous chemicals based on STAMP-HFACS combined model. Process Safety Progress, 44(4): 594-605. https://doi.org/10.1002/prs.70016
[7] Cvetković, V.M., Renner, R., Jakovljević, V. (2024). Industrial disasters and hazards: From causes to consequences—A holistic approach to resilience. International Journal of Disaster Risk Management, 6(2): 149-168. https://doi.org/10.18485/ijdrm.2024.6.2.10
[8] Lee, M.C. (2024). Comparison of consequence analysis results for a hydrogen fueled combined cycle power plant using ALOHA, E-CA and Hy-KoRAM Programs. Journal of the Korean Institute of Gas, 28(4): 90-104. https://doi.org/10.7842/kigas.2024.28.4.90
[9] Barjoee, S.S., Elmi, M.R., Varaoon, V.T., Keykhosravi, S.S., Karimi, F. (2022). Hazards of toluene storage tanks in a petrochemical plant: Modeling effects, consequence analysis, and comparison of two modeling programs. Environmental Science and Pollution Research, 29(3): 4587-4615. https://doi.org/10.1007/s11356-021-15864-5
[10] Hussain, N.K.H. (2024). The future scenarios for air quality and climate change. In Air Pollution, Air Quality, and Climate Change, Elsevier, pp. 249-271. https://doi.org/10.1016/C2023-0-01094-9
[11] Patel, O.P., Edwards, J.K., Kucharska-Newton, A.M., Whitsel, E.A., et al. (2026). Association of oil spill-related volatile organic compound exposure with CVD-related biomarkers in the Gulf Long-term Follow-up study. Annals of Work Exposures and Health, 70(1): wxaf091. https://doi.org/10.1093/annweh/wxaf091
[12] Yang, Y. (2025). A review of the application of unmanned aerial vehicles in air pollution monitoring. Advances in Engineering Innovation, 16(7): 142-149.
[13] Hu, Q., Qian, X., Shen, X., Zhang, Q., et al. (2022). Investigations on vapor cloud explosion hazards and critical safe reserves of LPG tanks. Journal of Loss Prevention in the Process Industries, 80: 104904. https://doi.org/10.1016/j.jlp.2022.104904
[14] Kim, S., Jang, T., Oli, T.,Park, C. (2023). Behavior of barrier wall under hydrogen storage tank explosion with simulation and TNT equivalent weight method. Applied Sciences, 13(6): 3744. https://doi.org/10.3390/app13063744
[15] Ding, Y., Zhang, X., Shi, Y., Zhang, H. (2022). Prediction of far-field blast loads from large TNT-equivalent explosives on gabled frames. Journal of Constructional Steel Research, 190: 107120 https://doi.org/10.1016/j.jcsr.2021.107120
[16] Wang, T., Huang, T., Hu, S., Li, Y., Yang, F., Ouyang, M. (2023). Simulation and risk assessment of hydrogen leakage in hydrogen production container. International Journal of Hydrogen Energy, 48(52): 20096-20111. https://doi.org/10.1016/j.ijhydene.2023.02.038
[17] Wang, S., Wang, G., Liu, D., Liu, C. (2022). Application of the improved vapor cloud explosion model to leakage explosion evaluation of high-pressure natural gas pipelines. Petroleum Science and Technology, 41(2): 214-229. https://doi.org/10.1080/10916466.2022.2042016
[18] Yang, J., Zhang, J., Hao, Q., Ren, J., Bi, M. (2026). Investigation on the combustion behavior and thermal radiation model of methanol pool fires under crosswind. International Journal of Heat and Mass Transfer, 261: 128592. https://doi.org/10.1016/j.ijheatmasstransfer.2026.128592
[19] Cirrone, D., Makarov, D., Molkov, V. (2023). Rethinking “BLEVE explosion” after liquid hydrogen storage tank rupture in a fire. International Journal of Hydrogen Energy, 48(23): 8716-8730. https://doi.org/10.1016/j.ijhydene.2022.09.114
[20] Cetinyokus, S. (2024). Determination of possible industrial accident effects on a hydrogen storage tank in a fuel cell production facility. Emergency Management Science and Technology, 4: e020. https://doi.org/10.48130/emst-0024-0020
[21] Duong, P.A., Lee, J., Kang, H. (2025). LPG dispersion in confined spaces: A comprehensive review. Engineering Reports, 7(3): e70064. https://doi.org/10.1002/eng2.70064
[22] Jindamanee, K., Keawboonchu, J., Pinthong, N., Meeyai, A., Inchai, P., Thepanondh, S. (2025). Environmental impacts and emission profiles of volatile organic compounds from petroleum refineries. Scientific Reports, 15(1): 15509. https://doi.org/10.1038/s41598-025-99932-7
[23] Khlaifat, A., El-Maghraby, R.M., Badawy, A.M. (2025). Quantitative assessment of fire and explosion hazards associated with propane and LPG pressurized storage tanks. Petroleum & Coal, 67(4): 1147.
[24] Xiao, H., Li, B., Yu, H., Shu, C.M. (2024). Dynamic risk analysis of hydrogen refueling station gas cloud explosions based upon the bow-tie perspective. International Journal of Hydrogen Energy, 82: 89-101. https://doi.org/10.1016/j.ijhydene.2024.07.353
[25] Wei, W.L., Chen, Y.Q., Wang, Z.Q., Li, S.T., Hang, C.L., Gao, Z. (2023). Research on damage effect of penetration and explosion integration based on volume filling method. International Journal of Impact Engineering, 177: 104591. https://doi.org/10.1016/j.ijimpeng.2023.104591
[26] Cheng, R., Chen, W., Hao, H., Li, J. (2022). Dynamic response of road tunnel subjected to internal Boiling liquid expansion vapour explosion (BLEVE). Tunnelling and Underground Space Technology, 123: 104363. https://doi.org/10.1016/j.tust.2022.104363
[27] Cheng, R., Chen, W., Hao, H., Li, J. (2023). Numerical prediction of ground vibrations induced by LPG boiling

liquid expansion vapour explosion (BLEVE) inside a road tunnel. Underground Space, 12: 44-64. https://doi.org/10.1016/j.undsp.2023.02.007
[28] Luan, T., Zhang, X., Chang, J., Wang, Y., Li, H. (2023). Dynamic risk analysis of flammable liquid road tanker based on fuzzy Bayesian network. Process Safety Progress, 42(4): 737-751. https://doi.org/10.1002/prs.12508
[29] Sheikhzadeh, G.A. (2024). Analysis of liquid gas (LPG) storage tank explosion in a road vehicle due to the boiling liquid vapor phenomenon (BLEVE). Modares Mechanical Engineering, 24(7): 421-431. https://doi.org/10.48311/mme.24.7.421
[30] Yang, Z., Li, C., Yan, Z., Zou, K., et al. (2025). Hazard analysis of parallel fueling of LOX/kerosene at space launch site: Accident scenario construction and lab-scale experiments. Fire Safety Journal, 157: 104487. https://doi.org/10.1016/j.firesaf.2025.104487
[31] Huffman, M., Hutchison, V., Ranganathan, S., Noll, G., Baxter, C., Hildebrand, M., Wang, Q. (2024). A comparative bibliometric study of the transport risk considerations of liquefied natural gas and liquefied petroleum gas. The Canadian Journal of Chemical Engineering, 102(6): 2019-2038. https://doi.org/10.1002/cjce.25226
[32] Min, M., Yoon, C., Yoo, N., Kim, J., Yoon, Y., Jung, S. (2025). Hydrogen risk assessment studies: A review toward environmental sustainability. Energies, 18(2): 229. https://doi.org/10.3390/en18020229
[33] Ricci, F., Ming, Y., Genserik, R., Cozzani, V. (2022). The role of emergency response in risk management of cascading events caused by Natech accidents. Chemical Engineering Transactions, 91: 361-366. https://doi.org/10.3303/CET2291061
[34] Xiong, S., Lv, W., Xiong, X., Liu, D., Li, X., Zhao, C. (2023). Research progress and application of emergency plans in China: A review. Emergency Management Science and Technology, 3(1): 1-16. https://doi.org/10.48130/EMST-2023-0003
[35] Ardila-Suarez, C., Lacoursière, J.P., Soucy, G., Rego de Vasconcelos, B. (2025). Consequence analysis of LPG-related hazards: Ensuring safe transitions to cleaner energy. Fuels, 6(2): 45. https://doi.org/10.3390/fuels6020045
[36] Cetinyokus, S., Gecer, C., Cetinyokus, T. (2025). Determination of safety distances for domino effects of process accidents in chemical organizations. Emergency Management Science and Technology, 5(1): e025. https://doi.org/10.48130/emst-0025-0023
[37] Cheng, W.H., Lin, C.H., Yuan, C.S. (2023). VOC sampler on a drone assisting in tracing the potential sources by a dispersion model—Case study of industrial emissions. Aerosol and Air Quality Research, 23(10): 230169. https://doi.org/10.4209/aaqr.230169
[38] Reindl, A.R., Olkowska, E., Pawłowski, J., Wolska, L. (2026). Occupational exposure to volatile organic compounds in polyurethane foam production—Concentration, variability and health risk assessment. Molecules, 31(1): 145. https://doi.org/10.3390/molecules31010145
[39] Badgujar, C.M., Zeedan, A. (2026). Quantitative risk assessment of gas-based combined cycle power plant using dispersion modeling. Process Safety Progress, 45(1): 45-58. https://doi.org/10.1002/prs.70042

NOMENCLATURE

ALOHA	areal locations of hazardous atmospheres
BLEVE	boiling liquid expanding vapour explosion
DRR	disaster risk reduction
ERPG	emergency response planning guidelines
IDLH	immediately dangerous to life or health
LEL	lower explosive limit
NNE	north-northeast
QRA	quantitative risk assessment
THF	tetrahydrofuran
TNT	trinitrotoluene
UEL	upper explosive limit
VCE	vapour cloud explosion
VOC	volatile organic compounds

Symbols

W_{tnt}	TNT equivalent mass of explosion (kg)
η	explosion efficiency factor (dimensionless)
m	mass of THF participating in explosion (kg)
Hc	heat of combustion of THF (kJ kg^{-1})
E_{tnt}	specific explosion energy of TNT (4184 kJ kg^{-1})
P_o	atmospheric pressure (101 kPa)
ΔP	peak overpressure generated by the explosion (kPa)
$R1$	structural damage radius (m)
$R2$	minor injury radius (m)
$R3$	fatal injury radius (m)

APPENDIX

Summary of key ALOHA model settings and input assumptions:

Table A1. ALOHA 5.4.7 model configuration used for reproducibility

Parameter	Configuration / Value
Software	ALOHA 5.4.7
Chemical	Tetrahydrofuran (THF), CAS 109-99-9
Toxic thresholds	ERPG-1: 100 ppm; ERPG-2: 500 ppm; ERPG-3: 5000 ppm; IDLH: 2000 ppm
Flammability limits	LEL: 20,000 ppm; UEL: 118,000 ppm
Study location	Izmit Port, Kocaeli-Izmit, Türkiye; elevation approximately 5 m
Meteorological condition	User-defined site-specific condition: wind 3 m/s from NNE at 10 m; air temperature 14 °C; relative humidity 68%; stability class C; cloud cover 4 tenths; no inversion height
Ground and building parameters	Open country ground roughness; concrete ground surface; ground temperature equal to ambient; building air exchange rate 0.57 h^{-1}
Storage tank configuration	Vertical cylindrical tank; volume 202 L; diameter 0.55 m; length 0.85 m; fill level 80%; THF mass 144 kg

Release configuration	Circular opening of 10 cm located at 0 m from tank bottom
Scenario 1 model	Leak from vertical cylindrical tank; flammable liquid escaping, not burning; Gaussian toxic vapor dispersion
Scenario 2 model	Thermal radiation from pool fire; ALOHA built-in solid-flame thermal radiation model; no manual heat of combustion or radiative fraction override
Scenario 3 model	BLEVE of flammable liquid in vertical cylindrical tank; 50% and 100% mass-in-fireball assumptions
Scenario 4 model	BLEVE of flammable liquid in horizontal cylindrical tank/road tanker; approximately 24 m^3 capacity, 80% fill, 17,144 kg THF; 50% and 100% mass-in-fireball assumptions
Thermal radiation thresholds	10.0 kW/m^2: potentially lethal within 60 s; 5.0 kW/m^2: second-degree burns within 60 s; 2.0 kW/m^2: pain within 60 s